ELSEVIER

Earth and Planetary Science Letters 146 (1997) E1–E7

EPSL

Express Letter

A Late Miocene–Pliocene origin for the Central Himalayan inverted metamorphism

T. Mark Harrison [a,*], F.J. Ryerson [b], P. Le Fort [c], An Yin [a], Oscar M. Lovera [a], E.J. Catlos [a]

[a] *W.M. Keck Foundation Center for Isotope Geochemistry, Department of Earth and Space Sciences and IGPP, University of California, Los Angeles, CA 90024, USA*

[b] *Lawrence Livermore National Laboratory, Livermore, CA 94550, USA*

[c] *Institut Dolomieu, C.N.R.S., Grenoble, 38301, France*

Received 24 September 1996; accepted 29 October 1996

Abstract

Perhaps the best known occurrence of an inverted metamorphic sequence is that found immediately beneath the Himalayan Main Central Thrust (MCT), generally thought to have been active during the Early Miocene. However, in situ $^{208}Pb/^{232}Th$ dating of monazite inclusions in garnet indicates that peak metamorphic recrystallization of the MCT footwall occurred in this portion of the central Himalaya at only ca. 6 Ma. The apparent inverted metamorphism appears to have resulted from activation of a broad shear zone beneath the MCT which tectonically telescoped the young metamorphic sequence. This explanation may resolve some outstanding problems in Himalayan tectonics, such why the MCT and not the more recently initiated thrusts marks the break in slope of the present day mountain range. It also renders unnecessary the need for exceptional physical conditions (e.g., high shear stress) to explain the generation of the Himalayan leucogranites.

Keywords: Main Central Thrust; metamorphism; Himalayas

1. Introduction

One of the best studied examples of the spatial association of intracontinental thrusting and inverted metamorphism, recognized in the Himalaya more than a century ago [1], is the sequence found immediately beneath the Main Central Thrust (MCT) (Fig. 1). Since all the major geologic elements of the Himalaya (i.e., leucogranites, South Tibet Detachment System (STDS), and inverted metamorphism; Fig. 1) have been related to the evolution of the MCT [2–4], establishing its slip history and variability along strike are key to understanding the nature of this orogenic belt. Although the question of a genetic link between Early Miocene anatexis in the MCT hanging wall and slip on the MCT and STDS is being debated [4–6], there has been no disagreement that Himalayan inverted metamorphism is temporally related to Early Miocene activity on the MCT.

The south-directed thrust faults of the Himalaya, principally the MCT and the Main Boundary Thrust,

* Corresponding author. Tel: +1 310 825 7970. Fax: +1 310 825 2779. E-mail: tmh@argon.ess.ucla.edu

PII S0012-821X(96)00215-4

sole in a common decollement at depth [7,8]. In general, the MCT places high-grade gneisses of the Tibetan Slab (= Greater Himalayan Crystallines) atop schists of the Midlands Formations (= Lesser Himalayan Formations), and the Main Boundary Thrust juxtaposes those schists against unmetamorphosed Neogene molasse (Fig. 1). Estimates of the amount of slip along the MCT vary between 140 and 300 km [9–11]. Geochronology of the MCT hanging wall indicates that deformation and anatexis were occurring at 22 ± 1 Ma, while cooling ages in the upper portion of the Tibetan Slab suggest that ductile deformation had ceased there by ~ 18 Ma [6,12,13].

Juxtaposition of the Tibetan Slab atop the Midlands along much of the Himalaya is associated with a zone of inverted metamorphism (Fig. 1, above). Proposed causes of the apparent increase in metamorphic grade with higher structural level include: thermal relaxation following nappe emplacement [7]; strain heating [14–16]; folding of pre-existing isograds [17]; imbricate thrusting [18]; mantle delamination [19]; and the ductile shearing of an existing zone of right-way-up metamorphism [20]. Within the central Himalaya, the Tibetan Slab increases in thickness from ~ 3 km in the Kali Gandaki section to > 10 km in the Burhi Gandaki section (Fig. 1). This correlates with an eastward increase in thickness and peak grade of the inverted metamorphic section, reaching corundum grade at Ankhu Khola (Fig. 1). The metamorphism within the Midlands (Fig. 1) typically increases in grade over a N–S distance of 10–20 km from chlorite through biotite, garnet, and kyanite, reaching sillimanite in the hanging wall [2]. The region approximately bounded by the garnet isograd and the MCT is typically characterized in the central Himalaya by a highly sheared, 4–8 km thick

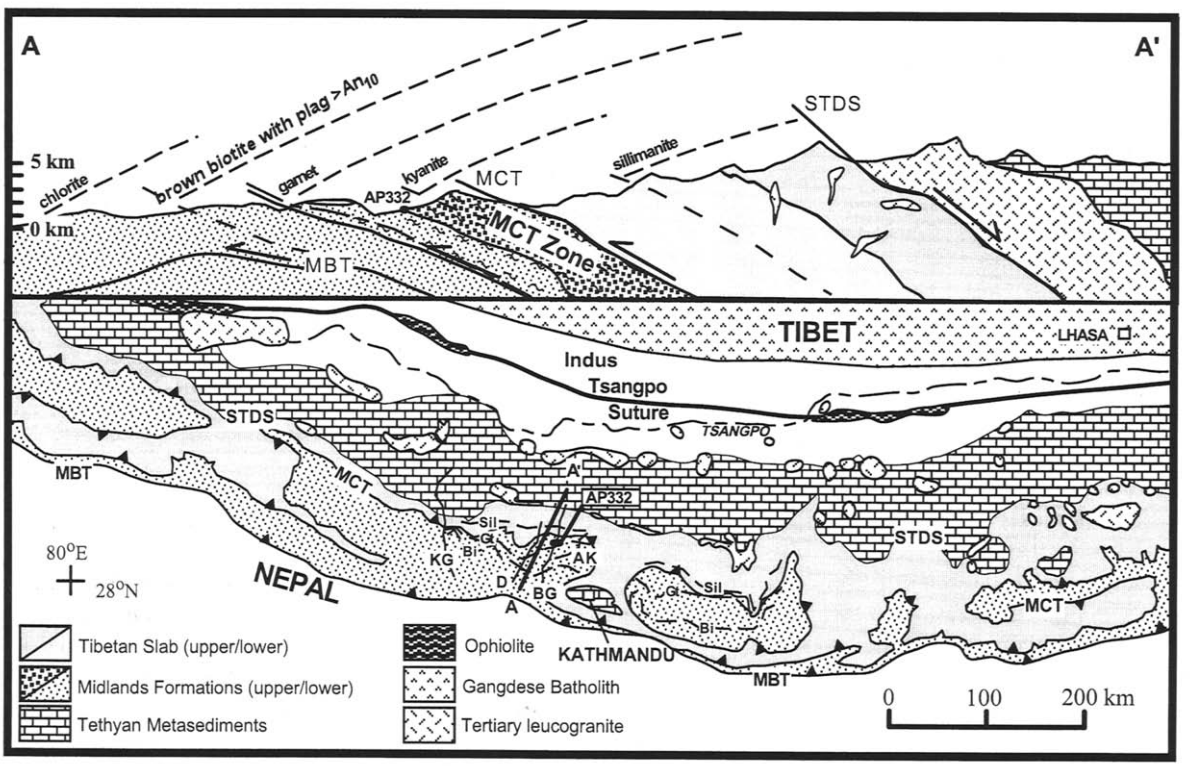

Fig. 1. Below: Geological sketch map of the Himalaya and Southern Tibet (after [3]) showing the relationship between the Tibetan Slab and Midlands Formations and reference isograds of the inverted metamorphic section. *MBT* = Main Boundary Thrust; *STDS* = Southern Tibetan Detachment System. The cross section marked A–A′ is shown in the inset. Sampled sections are: *KG* = Kali Gandaki; *BG* = Burhi Gandaki; *D* = Darondi Khola; *AK* = Ankhu Khola. Above: Generalized cross section through the central Himalaya (after [2]) illustrating the pattern of inverted metamorphism beneath the Main Central Thrust (MCT). The projected location of sample AP332 is shown.

zone of distributed deformation (Fig. 1) referred to as the "MCT zone" [20,21]. Abundant kinematic indicators within this broad zone document a uniformly top-to-the-south shear sense.

We examined the accessory mineralogy of pelites from the Midlands of central Nepal with the goal of using monazite to establish the timing of inverted metamorphism. Monazite is generally unstable in pelitic rocks during diagenesis and does not reappear until a temperature of ~500°C is reached [22,23]. Petrographic observations with the SEM indicate, that at chlorite and biotite grades, allanite is the principal host of LREE in these rocks. Monazite overgrowths begin to appear on allanite hosts close to the garnet isograd and ~10–50 micron-sized neoformed monazites are present within the garnet-grade rocks.

2. Results

Four monazite grains identified in a polished thin section of sample AP332 (Fig. 1) were dated in situ by the $^{208}Pb/^{232}Th$ ion microprobe method [6]. Those regions containing monazite were isolated by sawing and then mounted with a standard in an epoxy mount and Au coated for analysis. The relatively high $^{208}Pb^*$ abundances in even young monazites, coupled with the high ionization efficiency of Pb from monazite under O_2^- bombardment [6], permit Th–Pb age determinations to be made in a ~10 μm spot on a ca. 5 Ma specimen in ~20 min. Ages are determined by direct reference to monazite standard 554 (Table 1). The standard calibration has a typical reproducibility of ±2% [6].

Based on previous geochronologic studies of the Tibetan Slab [6,13], our expectation was that crystallization ages might range from ~20 to >30 Ma. Surprisingly, four different monazite grains yield $^{208}Pb/^{232}Th$ ages (Table 1) between 4.5 and 8.0 Ma. Excluding the latter age, these results yield a weighted mean of 5.62 ± 0.16 Ma (2σ; MSWD = 0.7). Of potentially greatest significance is a 15 μm × 50 μm monazite grain included within a millimetre-sized garnet in AP332, which yielded two Th–Pb measurements with an average apparent age of 5.6 ± 0.2 Ma. Garnet–biotite–plagioclase–muscovite–quartz thermobarometry [24,25] together with consideration of chlorite stability yields a P–T of 6–8 kbar and 550 ± 30°C, typical of conditions found within the MCT zone in this region [21]. Using experimentally determined diffusion parameters [26], we calculate the rate of diffusive Pb loss from a 15 μm thick monazite slab held at 550°C to be only ~10%/Ma. However, the ~4 Ma Ar closure ages of nearby biotites [12] constrains AP332 to have been <400°C since then, precluding the possibility of Pb^* loss since that time. These two lines of evidence thus restrict the *maximum* possible crystallization age of this monazite to no greater than 6 Ma.

Table 1
Th–Pb ion microprobe monazite ages for Buhri Gandaki pelite AP332

Grain	Spot	$^{208}Pb^*$ [a] (%)	$^{208}Pb/^{232}Th$ age [b] (Ma ± 2σ)
1	1	24	5.7 ± 1.4
1	2	84	8.0 ± 0.8
2	1	81	5.5 ± 0.4
2	2	87	5.7 ± 0.2
5	1	34	6.0 ± 1.8
6	1	28	4.6 ± 1.6
6	2	77	5.0 ± 0.6
6	3	80	5.5 ± 0.4

[a] Calculated assuming common $^{208}Pb/^{204}Pb = 39.5$ [32].
[b] Ages based on comparison with monazite 554 (= 45 Ma; $^{208}Pb/^{232}Th$ isotope dilution isochron; M. Tatsumoto, pers. commun., 1995).

Since the garnet and monazite isograds are nearly coincident in temperature (i.e., ~500°C), we conclude that these data are *prima facie* evidence that garnet growth in the presently exposed rocks was occurring at a depth of ~25 km at ~6 Ma. Measurements of monazite in garnets from Darondi Khola samples at a similar structural level (Fig. 1) typically yield 8–9 Ma ages which, although somewhat older than the range for AP332, are consistent with the pattern of inverted metamorphism in the central Himalaya being established during the Late Miocene.

Two other lines of evidence also suggest that MCT activity continued into the Pliocene. $^{40}Ar/^{39}Ar$ biotite ages [12] from section A–A′ (Fig. 1) drop from ~16 Ma in the upper MCT hanging wall to ~4 Ma within and adjacent to the MCT zone before climbing to pre-Tertiary ages (Fig. 2d). A U–Ti oxide precipitated in a zone of greenschist alteration

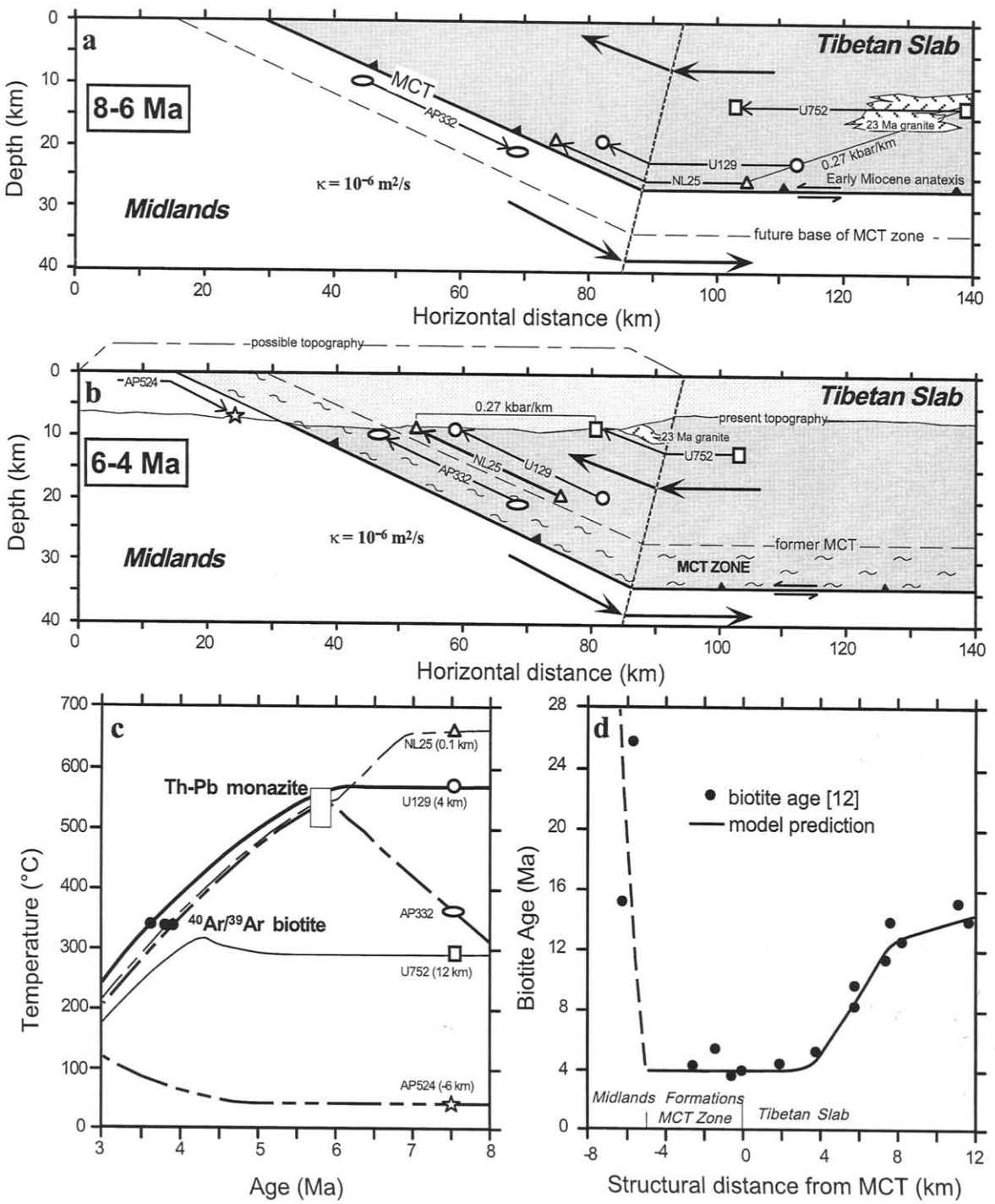
a
8-6 Ma
Tibetan Slab
MCT
AP332
U752
23 Ma granite
U129
0.27 kbar/km
NL25
Early Miocene anatexis
κ = 10⁻⁶ m²/s
Midlands
future base of MCT zone
Depth (km)
Horizontal distance (km)
b
possible topography
AP524
6-4 Ma
Tibetan Slab
0.27 kbar/km
present topography
23 Ma granite
U752
NL25
U129
AP332
κ = 10⁻⁶ m²/s
former MCT
MCT ZONE
Midlands
Depth (km)
Horizontal distance (km)
c
Th-Pb monazite
NL25 (0.1 km)
U129 (4 km)
40Ar/39Ar biotite
AP332
U752 (12 km)
AP524 (-6 km)
Temperature (°C)
Age (Ma)
d
biotite age [12]
model prediction
Midlands Formations
MCT Zone
Tibetan Slab
Biotite Age (Ma)
Structural distance from MCT (km)

within the Tibetan Slab yields U–Pb ages of 4.8–5.2 Ma [12]. Although these young ages were previously ascribed, respectively, to resetting and crystallization due to hypothesized hot fluids channelled along the MCT at 5 Ma [12], the ~ 7 kbar pressure for AP332 appears to rule this out. This is because both the upper portion of the Tibetan Slab and the lower grade portion of the Midlands are known from thermochronometry [12] to have been relatively cold, and therefore close (< 15 km) to the Earth's surface, at 5 Ma when AP332 was at ~ 25 km depth.

3. Discussion

The hypothesis that appears to best explain the existing data is that, following termination of a phase of slip along the MCT at ~ 20 Ma, the MCT was reactivated during the Late Miocene. Slip was initially restricted to the MCT fault and resulted in the burial metamorphism of the upper Midlands. Upward advection of heat within the hanging wall during transport up the ramp may have driven fluid circulation that produced the localized greenschist alteration [12]. Deformation subsequently moved from the fault to the broad underlying MCT shear zone, possibly due to the combined effects of surface uplift and erosion lowering the level of the brittle–ductile transition, resulting in the juxtaposition of two right-way-up metamorphic sequences. The magnitude of displacement across this ductile shear zone was sufficient to reorient the isograds into approximate parallelism with the shear zone boundaries [20].

We have consolidated our observations in the framework of a numerical model in order to illustrate possible Late Miocene/Pliocene deformation histories that are consistent with our thermobarochronologic result. We assume that the MCT initiated with a flat-ramp geometry and use a finite-difference solution to the diffusion–advection equation to examine P–T–t variations in the hanging wall and footwall as a result of thrusting. We assume a fixed fault geometry with respect to the surface and flexural-bending deformation in both hanging wall and footwall (boundary conditions and other model parameters are given in Fig. 2). For example, a rudimentary model which matches our isotopic constraints assumes that the MCT fault was reactivated at 8 Ma (following ~ 12 Ma of inactivity) with a slip rate of 22 mm/yr (Fig. 2a). At 6 Ma, activity shifted from the northern to the southern boundary of the MCT zone (Fig. 2b). Although the MCT zone is without question a broad (> 4 km) shear zone (Fig. 2a,b), for simplicity we have modeled it as a single fault at the base of the shear zone. In either case, the net effect is that garnet-grade Midlands rocks are accreted to the hanging wall, which continues to be transported up the ramp. Slip terminates at 4 Ma. Together with the kinetic parameters for Ar diffusion in biotite [27], the calculated thermal histories corresponding to mineral dating localities predict a biotite age distribution (solid curve, Fig. 2d) that match the empirical results [12]. More importantly, the model also predicts that the presently exposed upper Midlands would have reached the garnet isograd at ~ 6 Ma at a P–T of 7

Fig. 2. Thermal modelling was undertaken assuming a fault-bend fold geometry, with reflecting side boundaries and top and bottom boundaries maintained at constant temperatures of 25°C and 1025°C, respectively (i.e., initial thermal gradient is 25°C/km). For simplicity, friction and internal heating were neglected and constant surface elevation was maintained by denudation. In the simple model shown, both the hanging wall and footwall move at 11 mm/yr in opposite directions for a net slip rate of 22 mm/yr. (a) Slip along the MCT begins at 8 Ma. Hanging wall rocks are first transported along the flat and then up the ramp. NL25 (△), the sample closest to the MCT and thus at the highest peak pressure (~ 7 kbar), is the first to reach the MCT (see [12,28]). It is followed sequentially up the ramp by U129 (○) and U752 (□), with respective peak pressures ~ 6 kbar and ~ 4 kbar (see [12,28]). Between 8 and 6 Ma, sample AP332 experiences burial metamorphism due to overthrusting by the Tibetan Slab reaching 7 kbar. (b) At 6 Ma, the MCT zone (modeled as a single fault at the base of the shear zone) is activated accreting the garnet grade Midlands rocks, formed by thrusting beneath the Tibetan Slab, into the hanging wall which continues to be transported up the ramp. Slip terminates at 4 Ma. Note that the three reference samples reach the surface preserving their original lithostatic gradient of 0.27 kbar/km [28]. (c) Temperature histories predicted by the thermal model for Tibetan Slab samples NL25, U129, U752, MCT zone sample AP332, and sample AP524 from beneath the MCT zone. The model predicts that the exposed MCT zone would have reached the garnet isograd at ~ 6 Ma at a P–T of 7 kbar and 550°C, in agreement with AP332 result (Table 1). (d) Biotite ages from a N–S traverse across the MCT zone and into the Tibetan Slab [12]. The thermal histories calculated by the numerical model predict biotite ages (curve) that closely match the observed distribution.

kbar and 550°C, in excellent agreement with the monazite-in-garnet result for AP332 (Fig. 2c).

Thermobarometry of rocks collected in the Tibetan Slab along section A–A′ (Fig. 1) indicate that pressures as high as ~ 7 kbar were achieved adjacent to the MCT, whereas peak pressures at the top of the section were only ~ 3–4 kbar [28]. When pressure is plotted against inferred structural height above the MCT, which dips 30°N, these results yield a "normal" lithostatic gradient of 0.27 kbar/km [28] implying that these rocks were once sub-vertical and subsequently rotated ~ 30°. Our model predicts that hanging wall rocks from the range of depths corresponding to these pressures would today be exposed at the surface together, as a result of the rotation associated with their sequential transport up the ramp (Fig. 2a,b). Although we emphasize that the results of our thermal modelling are not unique, particularly with respect to the timing of reactivation of the MCT, they demonstrate both the physical plausibility of our hypothesis and that a wide variety of observations can be reconciled within its framework.

If Late Miocene activation of the MCT zone and the subsequent development of inverted metamorphism were widespread within the central Himalaya, two long-standing geodynamic and geomorphological puzzles may be resolved. The MCT zone marks the most dramatic break in slope within the Himalaya whereas the more recently activated thrusts are topographically subdued [29]. If the MCT had been largely inactive for the past ~ 20 Ma, why would this feature persist? Although a shallow (~ 15°) ramp at ~ 20 km depth on the decollement [30] may contribute to elevating the MCT zone, it would not be expected to produce a sharp break in slope over such a short distance in rocks of normal flexural strength. The break in slope may simply reflect that significant displacement along the MCT zone was occurring as recently as 4 Ma.

The many attempts to account for the thermal energy required by Tibetan Slab anatexis all share a common element: each calls on an extraordinary process to have aided melting. The mechanisms that have been proposed include: high (> 100 MPa) shear stress on the MCT [16], very long (> 25 Ma) or short (≤ 1 Ma) thermal incubation [16], high erosion rates coupled with high heat production [31], tectonic decompression [5], and mantle delamination [19]. Although the juxtaposition of rocks experiencing partial melting against the relatively cold rocks of the MCT zone undergoing endothermic reactions [7] appears enigmatic, our hypothesis provides a simple explanation.

Although refrigeration due to underthrusting is an important factor along the ramp [15], its role as a heat sink is significantly diminished on the thrust flat. At locations distant from the ramp vertex, a relatively small shear stress (~ 30 MPa) along the fault can generate enough frictional heating to locally increase temperatures to produce anatexis. We speculate that the ca. 20 Ma leucogranites were produced under these conditions and that the (presumably higher grade) footwall rocks that were then juxtaposed against the thrust flat of the MCT have since been displaced northward and replaced by a tectonically telescoped section of lower grade rocks on the ramp. Consequently, any attempt to explain the present juxtaposition of the Tibetan Slab against the Midlands Formations without recognizing the diachroneity of deformation will require an appeal to some extraordinary process or circumstance.

Acknowledgements

We thank Kevin McKeegan and Chris Coath for their help with the isotopic measurements, Dan Farber for SEM characterization of AP332, Frank Spear and Trevor Ireland for constructive reviews, and NSF for support. *[FA]*

References

[1] R.D. Oldham, The geology of Jaunsar and the Lower Himalayas, Rec. Geol. Surv. India 16, 193–198, 1883.

[2] M. Colchen, P. Le Fort and A. Pêcher, Annapurna–Manaslu–Ganesh Himal notice de la carte geologiquie au 1/200,000e, Bilingual edition: French–English. Centre Natl. Rech. Sci., Paris, 1986.

[3] P. LeFort, M. Cuney, C. Deniel, C. France-Lanord, S.M.F. Sheppard, B.N. Upreti and P. Vidal, Crustal generation of the Himalayan leucogranites, Tectonophysics 134, 39–57, 1987.

[4] B.C. Burchfiel, Z. Chen, K.V. Hodges, Liu Y., L.H. Royden, C. Deng and J. Xu, The South Tibetan Detachment System, Himalayan Orogen: Extension contemporaneous with and parallel to shortening in a collisional mountain belt, GSA Spec. Pap. 269, 41 pp., 1992.

[5] N. Harris and J. Massey, Decompression and anatexis of Himalayan metapelites, Tectonics 13, 1537–1546, 1994.
[6] T.M. Harrison, K.D. McKeegan and P. LeFort, Detection of inherited monazite in the Manaslu leucogranite by $^{208}Pb/^{232}Th$ ion microprobe dating: Crystallization age and tectonic significance, Earth Planet. Sci. Lett. 133, 271–282, 1995.
[7] P. Le Fort, Himalayas, the collided range. Present knowledge of the continental arc, Am. J. Sci. 275A, 1–44, 1975.
[8] W. Zhao, K.D. Nelson and Project INDEPTH, Deep seismic reflection evidence for continental underthrusting beneath southern Tibet, Nature 366, 557–559, 1994.
[9] H. Lyon-Caen and P. Molnar, Gravity anomalies, flexure of the Indian plate, and the structure, support and evolution of the Himalaya and the Ganga Basin, Tectonics 4, 513–538, 1985.
[10] D. Schelling and K. Arita, Thrust tectonics, crustal shortening, and the structure of the far-eastern Nepal, Himalaya, Tectonics 10, 851–862, 1991.
[11] P. Srivastava and G. Mitra, Thrust geometries and deep structure of the outer and lesser Himalaya, Kumaon and Garwal (India): Implications for evolution of the Himalayan fold-and-thrust belt, Tectonics 13, 89–109, 1994.
[12] P. Copeland, T.M. Harrison, K.V. Hodges, P. Maréujol, P. LeFort and A. Pêcher, An Early Pliocene thermal perturbation of the Main Central Thrust, Central Nepal: Implications for Himalayan tectonics, J. Geophys. Res. 96, 8475–8500, 1991.
[13] R.R. Parrish and K.V. Hodges, Miocene (22 ± 1) Ma metamorphism and two stage thrusting in the Greater Himalayan Sequence, Annapurna Sanctuary, Nepal, GSA Abstr. Programs 25, A174, 1993.
[14] K. Arita, Origin of the inverted metamorphism of the Lower Himalaya, central Nepal, Tectonophysics 95, 43–60, 1983.
[15] P. England and P. Molnar, The interpretation of inverted metamorphic isograds using simple physical calculations, Tectonics 12, 145–157, 1993.
[16] P. England, P. Le Fort, P. Molnar and A. Pêcher, Heat sources for Tertiary metamorphism and anatexis in the Annapurna–Manaslu region, Central Nepal, J. Geophys. Res. 97, 2107–2128, 1992.
[17] M.P. Searle and D.C. Rex, Thermal model for the Zanskar Himalaya, J. Metamorph. Geol. 7, 127–134, 1989.
[18] M. Brunel and J.R. Kienast, Étude pétro-structurale des chevauchments ductiles himalayens sur la transersale de L'Everest–Makalu (Népal oriental), Can. J. Earth Sci. 23, 1117–1137, 1986.
[19] P. Bird, Initiation of intracontinental subduction in the Himalaya, J. Geophys. Res. 83, 4975–4987, 1978.
[20] M.S. Hubbard, Ductile shear as a cause of inverted metamorphism: example from the Nepal Himalaya, J. Geol. 104, 493–499, 1996.
[21] A. Pêcher, The metamorphism in the central Himalaya, J. Metamorph. Petrol. 7, 31–41, 1989.
[22] H.A. Smith and B. Barreiro, Monazite U–Pb dating staurolite-grade metamorphism in pelitic shists, Contrib. Mineral. Petrol. 105, 602–615, 1990.
[23] J.A. Kingsbury, C.F. Miller, J.L. Wooden and T.M. Harrison, Monazite paragenesis and U–Pb systematics in rocks of the eastern Mojave Desert, California, U.S.A.: implications for thermochronometry, Chem. Geol. 110, 147–168, 1993.
[24] K.V. Hodges and F.S. Spear, Geothermometry, geobarometry and the Al_2SiO_5 triple point at Mt. Moosilauke, New Hampshire, Am. Mineral. 67, 1118–1134, 1982.
[25] K.V. Hodges and P.D. Crowley, Error estimation and empirical geothermobarometry for pelitic systems, Am. Mineral. 70, 702–709, 1985.
[26] H.A. Smith and B.J. Giletti, Pb diffusion in monazite, Geochim. Cosmochim. Acta, in press, 1996.
[27] M. Grove and T.M. Harrison, ^{40}Ar diffusion in Fe-rich biotite, Am. Mineral. 81, 940–951, 1996.
[28] K.V. Hodges, P. Le Fort and A. Pêcher, Possible thermal buffering by crustal anatexis in collisional orogens: Thermobarometric evidence from the Nepalese Himalaya, Geology 16, 707–710, 1988.
[29] J.G. Masek, B.L. Isacks, T.L. Gubbels and E.J. Fielding, Erosion and tectonics at the margins of continental plateaus, J. Geophys. Res. 99, 13,941–13,956, 1994.
[30] R.S. Yeats, Slip rate and earthquake recurrence interval on Himalayan plate-boundary megathrust, Abstracts of the 11th Himalayan–Karakorum–Tibet Workshop, Flagstaff, AZ, April 29–May 1, 1996, pp. 171–172, 1996.
[31] L.H. Royden, The steady state thermal structure of eroding orogenic belts and accretionary prisms, J. Geophys. Res. 98, 4487–4507, 1993.
[32] C. Deniel, P. Vidal, A. Fernandez, P. Le Fort and J.J. Peucat, Isotopic study of the Manaslu granite (Himalaya, Nepal): inferences on the age and source of the Himalayan leucogranites, Contrib. Mineral. Petrol. 96, 78–92, 1987.